



First stage of Antarctic ozone recovery

E.-S. Yang,^{1,2} D. M. Cunnold,¹ M. J. Newchurch,³ R. J. Salawitch,^{4,5} M. P. McCormick,⁶ J. M. Russell III,⁶ J. M. Zawodny,⁷ and S. J. Oltmans⁸

Received 4 December 2007; revised 2 July 2008; accepted 18 July 2008; published 21 October 2008.

[1] Ozone within the springtime Antarctic vortex is affected by both chemical and dynamical processes. We use correlations between monthly means of total ozone columns and temperatures in the vortex core and the vortex edge (or collar) regions to construct ozone anomaly time series for September and October, which mainly reflect variations in ozone due to chemical forcing. The ozone anomaly time series, obtained from ground-based Dobson/Brewer column measurements, reveal a statistically significant leveling off of total ozone, relative to the previous rate of decline, since 1997. The second derivative with respect to time of stratospheric halogen loading in the Antarctic vortex reached a well-defined minimum in 1997, marking the time when the chemical forcing of polar ozone loss started leveling off. Vertical profiles of ozone in the Antarctic vortex from SAGE II and ozonesondes show that near-zero levels of ozone have sometimes been reached in the core of the vortex each October, between the 380 and 500 K isentropes, since 1992. We have accounted for this so-called loss saturation effect in our analysis by comparing the frequency distribution of measured ozone with the distribution expected from a reconstruction of ozone that hypothetically allows ozone abundances to drop below zero. This approach indicates that changes in stratospheric halogen loading, not the loss saturation effect, are the primary cause of the recent leveling off of the total ozone anomaly time series. This analysis indicates that total column ozone within the Antarctic vortex core and collar regions has reached the first stage of recovery as defined by the World Meteorological Organization: a statistically significant reduction in the rate of decline that is clearly attributable to decreases in the abundance of ozone-depleting substances brought about by the Montreal Protocol.

Citation: Yang, E.-S., D. M. Cunnold, M. J. Newchurch, R. J. Salawitch, M. P. McCormick, J. M. Russell III, J. M. Zawodny, and S. J. Oltmans (2008), First stage of Antarctic ozone recovery, *J. Geophys. Res.*, *113*, D20308, doi:10.1029/2007JD009675.

1. Introduction

[2] Over the past 2 decades, the Antarctic ozone hole [Farman *et al.*, 1985] has been a global environmental problem of great significance [e.g., Solomon, 1999; World Meteorological Organization (WMO), 2007, and references therein]. The association of polar ozone depletion with anthropogenic chlorine and bromine led to the passage of the Montreal Protocol and its amendments that at first

limited, and then essentially banned, a wide range of industrial chlorine and bromine (halogen) compounds that cause ozone depletion [e.g., WMO, 2007, section 4.0]. The reduction in stratospheric halogen loading brought about by this legislation will eventually lead to the full recovery of the Antarctic ozone hole, which will occur sometime in the middle of this century [Austin and Wilson, 2006; Newman *et al.*, 2006; WMO, 2007, Chapter 6]. Recently, it has become apparent that the Antarctic ozone hole affects wind patterns throughout the southern hemisphere troposphere and also affects the temperature of the southern polar region such that the recovery of the ozone hole may drive surface warming of the Antarctic continent [Perlwitz *et al.*, 2008; Son *et al.*, 2008].

[3] Our paper is focused on identification of the *first stage* of recovery of the Antarctic ozone hole. This stage is defined as the occurrence of a statistically significant reduction in the rate of ozone decline that is clearly attributable to changes in the abundance of ozone depleting substances [WMO, 2007, Chapter 6]. Bodeker *et al.* [2002] showed that the size of the Antarctic ozone hole, with total column ozone less than 220 Dobson units (1 DU = 0.001 atm cm), steadily increased over the 1979 to 2000 time period, coincident with rising levels of stratospheric halogens. Newman *et al.*

¹School of Earth and Atmospheric Sciences, Georgia Institute of Technology, Atlanta, Georgia, USA.

²Now at Earth Systems Science Center, University of Alabama in Huntsville, Huntsville, Alabama, USA.

³Atmospheric Science Department, University of Alabama in Huntsville, Huntsville, Alabama, USA.

⁴Jet Propulsion Laboratory, California Institute of Technology, Pasadena, California, USA.

⁵Now at Department of Atmospheric and Oceanic Sciences, University of Maryland, College Park, Maryland, USA.

⁶Center for Atmospheric Sciences, Hampton University, Hampton, Virginia, USA.

⁷NASA Langley Research Center, Hampton, Virginia, USA.

⁸NOAA Earth System Research Laboratory, Boulder, Colorado, USA.

[2004, 2006] showed that long-term changes in the size of the ozone hole (after removal of year-to-year fluctuations due to meteorological conditions) bear a close relation to variations in stratospheric halogen loading. *Huck et al.* [2007] showed that the long-term trend of ozone mass deficit within the ozone hole followed a pattern similar to that of stratospheric halogens, with strong interannual variability (due to meteorological conditions) apparent in recent years. No prior study, however, has provided quantitative analysis showing that changes in ozone within the core of the Antarctic vortex are consistent with the first stage of recovery.

[4] The identification of the first stage of ozone recovery is complicated by two factors, both of which are considered in quantitative detail by our analysis:

[5] 1. The size and depth of the ozone hole is sensitive to year-to-year variations in meteorological conditions [e.g., *Lee et al.*, 2001; *Newman et al.*, 2004]. Indeed, the ozone hole was relatively small and the minimum ozone column was relatively high in 2002 due to an anomalous early warming [e.g., *Allen et al.*, 2003; *Newman et al.*, 2006]. In contrast, the 2006 ozone hole was relatively large and minimum ozone column was at a record low, due to weak planetary wave activity that resulted in a cold, isolated vortex [*Massom et al.*, 2008]. Any assessment of recovery must account for dynamical variability of ozone depletion.

[6] 2. Ozone loss saturation: essentially all ozone is destroyed for particular altitude regions over Antarctica during October. Levels of ozone indistinguishable from zero were first observed in the Antarctic vortex during October 1992 [*Hofmann et al.*, 1994; *Hofmann et al.*, 1997]. If ozone loss saturates at particular altitudes, then the “leveling off” of column ozone could be due to the fact that the atmosphere has simply “run out” of ozone that can be depleted. Any assessment of recovery must also account for the saturation of ozone loss in a quantitative manner.

[7] *Yang et al.* [2005] examined long-term changes of ozone in the edge (collar) region of the Antarctic vortex, between 60° and 70°S geographic latitude, during September and October. After accounting for dynamical variations and loss saturation, they concluded that the flattening of ozone loss in the Antarctic collar region was consistent with the leveling off of stratospheric halogen loading. In contrast, *Solomon et al.* [2005] asserted that ozonesonde measurements at the Syowa (69°S) and South Pole stations did not indicate ozone recovery associated with changing stratospheric halogen loading. This disagreement may not be as contradictory as it first appears because *Solomon et al.* [2005] defined recovery as “the degree to which changes in emissions of ozone-depleting source gases such as CFCs are reflected in improvements in the state of the ozone layer.” Moreover, *Yang et al.* [2005] focused on the collar region of the vortex (60–70°S); whereas *Solomon et al.* [2005] used ozone measurements mostly from inside the vortex (poleward of 69°S). A consistent quantification of the Antarctic ozone depletion, which covers both the vortex core and collar regions, is needed.

[8] Our present study extends the work of *Yang et al.* [2005] by providing separate analyses of ozone time series for both the vortex core and collar regions. Equivalent latitude, defined based on gradients of potential vorticity (PV) on surfaces of constant potential temperature

(isentropes), is used to distinguish these regions (*Yang et al.* [2005] had used only geographic latitude). Particular emphasis is given to data collected in the core of the Antarctic vortex. We use correlations between year-to-year residuals in ozone and temperature to arrive at an ozone time series that has been adjusted to account for yearly variations in ozone due to meteorological conditions.

[9] We highlight details of the two time periods that play an essential role in our study. The first period marks the time when we would expect to see a statistically significant reduction in the rate of decline of the chemical loss of Antarctic ozone. Chemical loss of polar ozone is driven by catalytic cycles limited by the reactions $\text{ClO} + \text{ClO}$ and $\text{BrO} + \text{ClO}$ [e.g., *WMO*, 2007, Chapter 4]. Total loss responds to stratospheric halogen loading in a nonlinear manner [e.g., *Jiang et al.*, 1996]. Studies of Antarctic ozone typically relate changes in ozone mass deficit [e.g., *Huck et al.*, 2007], ozone anomalies [e.g., *Yang et al.*, 2005], or the size of the ozone hole [e.g., *Newman et al.*, 2006] to variations in equivalent effective stratospheric chlorine (EESC), which combines Cl_y and total organic bromine (Br_y) into a single quantity that represents the relative contributions of chlorine and bromine to ozone loss. *Newman et al.* [2006] first described equivalent effective Antarctic stratospheric chlorine (EEASC), a version of EESC specific to the Antarctic vortex. The quantity EEASC has a longer mean age of air, greater width of age of air spectrum, and larger weighting of Br_y relative to the values of these parameters commonly used in the formulation of EESC [*Newman et al.*, 2006].

[10] Figure 1 shows time series of EEASC and EESC. The time series of EEASC used here has a mean age of 6 years, an age spectrum width of 3 years, and a bromine scaling factor (α) of 65. It is based on time series for Cl_y and Br_y from the A1 scenario of *WMO* [2007]. All quantities originate from *WMO* [2007, Chapter 8]. Figure 1 compares this EEASC time series to two similar versions of EEASC used by *Newman et al.* [2006], which differ slightly in the specification of age of air, spectrum width, and α . Also shown, for comparison, is a curve for EESC. Figure 1 also shows first and second derivatives of EEASC and EESC. A well-defined minimum in the second derivative of EEASC occurs at the start of year 1997, as indicated. This means that the rate of change of stratospheric halogens in the Antarctic vortex was changing more rapidly, at this time, than at any other time. Assuming changes in chemical ozone loss are driven by variations in halogen loading, early 1997 is the time when we would expect to see the largest change in the rate of polar ozone depletion. Our study focuses only on detecting change in ozone trend (first stage of ozone recovery), and does not focus on detecting a turnaround of ozone depletion occurring at a maximum EEASC (second stage of ozone recovery). Hence, for purposes of trend analysis, we group our data into two time periods: “1979 to 1996” and “1997 to 2007,” reflecting the importance of early 1997 as the time when we would expect to see the most dramatic change in the rate of decline of ozone depletion.

[11] In our analysis of ozone trends, data collected in 1982 as well as 1992 and 1993 are not used, due to the influence on polar ozone of aerosols associated with the eruptions of El Chichón (March–April 1982) and Mount

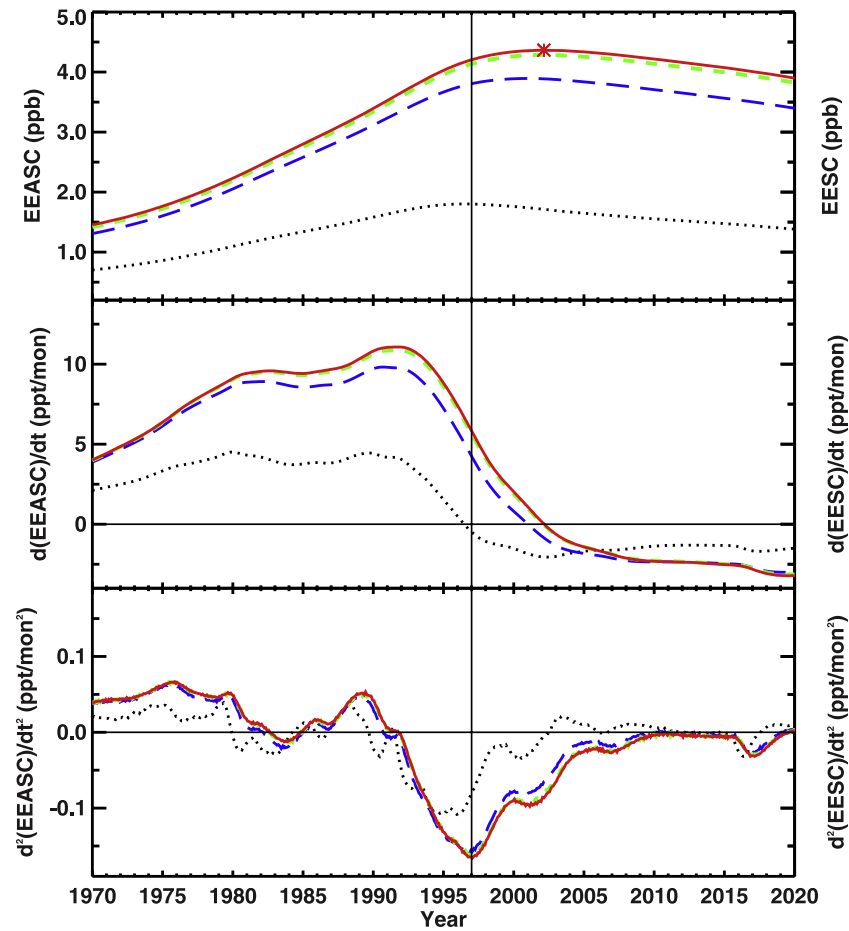


Figure 1. Equivalent effective Antarctic stratospheric chlorine (EEASC) (red, blue, and green curves) and equivalent effective stratospheric chlorine (EESC) (black curve) versus (top) time, (middle) the first derivative of EEASC and EESC, and (bottom) the second derivative of EEASC and EESC. For all curves, the age spectrum width [Waugh and Hall, 2002] has been set equal to one half of the mean age, a common approach for estimates of stratospheric halogen loading [e.g., Newman *et al.*, 2006]. The red solid curve shows EEASC used in this study: mean age of air of 6 years and bromine scaling factor (α) of 65 (this value for α , based on the work of Chipperfield and Pyle [1998], is recommended by WMO [2007] for use in the formulation of EEASC). The blue long-dashed curve shows the primary EEASC relation used by Newman *et al.* [2006]: mean age of 5.5 years and $\alpha = 50$. The green short-dashed curve shows another EEASC relation discussed by Newman *et al.* [2006]: mean age of 6 years and $\alpha = 60$. The black dotted curve shows values for EESC (a halogen loading scenario appropriate for midlatitude air parcels) used in past ozone assessments: mean age of 3 years and $\alpha = 45$. The curves for EEASC and EESC are based on the formulation described by Newman *et al.* [2006] and illustrated in box 8–1 of WMO [2007]. Numerical values were obtained from a Web site designed and maintained by P. A. Newman: http://code916.gsfc.nasa.gov/Data_Services/automailer/index.html (click on “EESC time series” icon). The vertical line denotes 1 January 1997. The asterisk on the red solid curve denotes the maximum of EEASC, which occurred in February 2002.

Pinatubo (June 1991) [Hofmann and Oltmans, 1993]. Analyses of ozone trends typically do not consider data collected during these years [Weatherhead and Andersen, 2006]. However, for convenience, we still denote the time periods as “1979 to 1996” and “1997 to 2007,” even though data obtained in 1982, 1992, and 1993 are not used in the analysis.

[12] Early 1997 is a robust marker for the first stage of polar ozone recovery. Various choices for the age of air, spectrum width, and bromine efficiency (all arguably appropriate for the polar vortex) lead to differences in EEASC (Figure 1) that have important consequences for

the projection of the date of the eventual long-term, full recovery of Antarctic ozone [Austin and Wilson, 2006; Newman *et al.*, 2006]. However, all of these curves exhibit minimum second derivatives in early 1997. When these three parameters are changed to values appropriate for the midlatitude lower stratosphere, the minimum in the second derivative of EESC occurs several years earlier (Figure 1), indicating the first stage of ozone recovery for the extrapolar, midlatitude lower stratosphere might be expected to have occurred prior to the first stage of recovery of polar ozone (of course, the sensitivity of midlatitude ozone to aerosols and year-to-year variations in transport would play

an important role in any study of ozone recovery for this region of the atmosphere). Finally, we note that upper stratospheric total chlorine, which is straightforward to quantify because nearly all of the chlorine is in the form of hydrogen chloride (HCl), is decreasing in a manner that is quantitatively consistent with calculations of EESC for this region of the atmosphere [Anderson *et al.*, 2000; Froidevaux *et al.*, 2006]. Hence, we have confidence that the changes in halogen loading predicted by EESC and EEASC are indeed being realized in the stratosphere.

[13] The second important time period denotes the time when Antarctic ozone showed signs of saturation of chemical loss. Observations of ozone in the core of the vortex at the South Pole, obtained during October 1991 and earlier years, show low but nonzero levels of ozone at all altitudes [Hofmann *et al.*, 1992] (also see Hofmann *et al.* [1997, Figure 6], who present time series of Antarctic ozone from 1986 to 1996). As noted above, ozone abundances indistinguishable from zero were first observed over a significant range of altitudes in the Antarctic vortex during October 1992 [Hofmann *et al.*, 1994, 1997]. The large increase in ozone depletion in 1992 compared to the prior year was due in part to the dramatic increase in aerosol loading associated with the eruption of Mount Pinatubo [Hofmann and Oltmans, 1993]. In September and October 1994, aerosol levels in the Antarctic vortex dropped considerably compared to prior years [Nardi *et al.*, 1997], yet ozone was observed to be essentially zero between 16 and 18 km in the core of the vortex [Hofmann *et al.*, 1997]. Values of ozone close to zero were also observed in regions of the vortex in 1995 and 1996 [Bevilacqua *et al.*, 1997; Nardi *et al.*, 1997] and in subsequent years [Nardi *et al.*, 1999] (loss saturation for all of these years is evident in data presented in section 5). For our analysis of ozone loss saturation, we consider the following two time periods: “1979 to 1991” and “1994 to 2007.” This designation reflects the facts that levels of ozone indistinguishable from zero have been observed for an appreciable range of altitudes from 1992 onward and that data collected during 1992 and 1993 are not considered, due to the presence of volcanic aerosols. Data collected in 1982 are also excluded from the analysis, but we refer to the early time period as “1979 to 1991.”

[14] We account quantitatively for the effect of ozone loss saturation for the time period from 1994 to 2007. The severe ozone hole of 2006 is also discussed in terms of loss saturation and the specific meteorological conditions of that year. Our analysis indicates that ozone levels within both the core and collar region of the Antarctic vortex, when adjusted for dynamical variations and loss saturation, has undergone a statistically significant reduction in the rate of decline (this conclusion is based on propagation of the linear, downward decline in ozone for the 1979 to 1996 time period onto data collected from 1997 to 2007). We also show that over the entire time period under consideration (i.e., 1979 to 2007), ozone levels within the Antarctic vortex follow a temporal variation that is well described by EEASC.

2. Data

[15] This analysis uses measurements of total ozone column from the Dobson/Brewer spectrophotometers in the southern hemisphere from the World Ozone and Ultravi-

olet Data Center (WOUDC, <http://www.msc-smc.ec.gc.ca/woudc>) as well as those at Vernadsky and Halley Bay from the British Antarctic Survey (BAS, <http://www.antarctica.ac.uk/met/jds/ozone>). Because the location of the edge of the polar vortex changes over time, we obtain the total column ozone data in the polar vortex core and collar region from 24 stations within the geographic latitude range of 30–90°S: Macquarie Island, Halley Bay, Buenos Aires, Hobart, Syowa, Amundsen-Scott, Invercargill, King Edward Point, Vernadsky/Faraday, Marambio, Lauder, Arrival Heights/McMurdo, Belgrano II, Scott Base, Ushuaia, Comodoro Rivadavia, Salto, King George Island, Ushuaia II, Maitri, Doctor Sobral, San Martin, Punta Arenas, and Zhongshan (of course, the polar vortex never extends anywhere close to 30°S, but we use all data poleward of this latitude for completeness). The selected data cover almost every day in September and October for the 1979 to 2007 time period. Vertical ozone profiles are obtained from ten ozonesonde stations (WOUDC and NOAA/ESRL): Macquarie Island, Mirny, Syowa, Amundsen-Scott, Marambio, Lauder, Novolaskarskaya/Forster, Neumayer, Maitri, and Davis. Vertical profiles of ozone are also obtained from the Stratospheric Aerosol and Gas Experiment II (SAGE II, <http://www-sage2.larc.nasa.gov>) and Halogen Occultation Experiment (HALOE, <http://haloedata.larc.nasa.gov>) measurements. Profiles of PV for potential temperature levels between 320 to 700 K, equivalent latitudes (for definition, see Butchart and Remsburg [1986]), and locations of the vortex edge are all calculated from the 6-hourly National Centers for Environmental Prediction (NCEP) temperature and wind data (<http://www.cdc.noaa.gov/cdc/reanalysis>).

3. Ozone in Equivalent Latitude Coordinates

[16] Potential vorticities derived from the NCEP reanalysis data set were linearly interpolated both horizontally and temporally to match the time and location of each ozone measurement. The horizontal winds, ozone abundances, and PV values were also interpolated onto isentropes from the 17 NCEP pressure levels. The 440 K isentrope (about 17 km for the Antarctic vortex) is especially important for our study because the maximum contribution to loss of column ozone originates from ozone depletion between 16 and 18 km [Hofmann *et al.*, 1997]. The equivalent latitude of each total ozone column measurement is calculated based on the PV values on the 440 K isentrope. The location of the vortex edge was based on the location of the maximum of the product of the latitudinal gradient of PV and the isentropic horizontal wind, and the poleward as well as equatorward boundaries of the vortex edge region were defined using the curvature of PV [Nash *et al.*, 1996].

[17] Figure 2 shows a time series of ozonesonde measurements of partial ozone columns and coincident temperatures on the 440 K (~70 hPa or ~17 km), 500 K (~50 hPa or ~19 km) and 600 K (~30 hPa or ~23 km) surfaces, inside the Antarctic polar vortex from 1986 to 2007. It is evident that variations of ozone and temperature are correlated. Moreover, the temperatures on the 440 K, 550 K and 600 K surfaces are strongly related to each other. For example, temperature variations at 440 and 600 K have correlation coefficients of 0.80 and 0.92, respectively, for

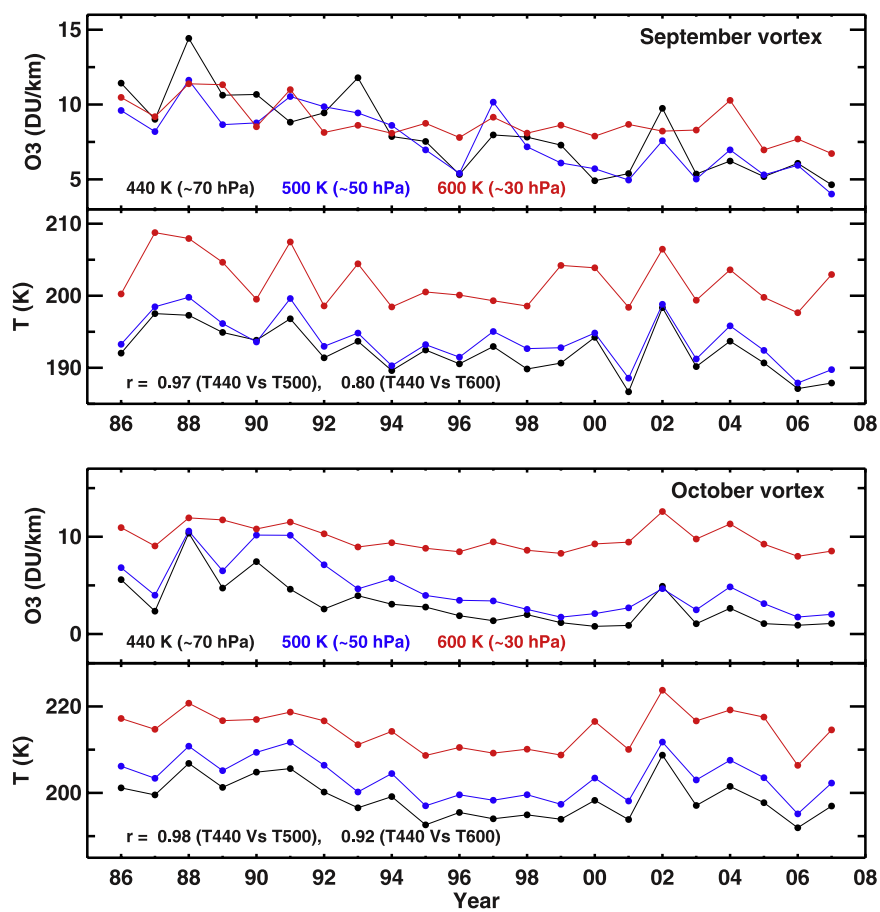


Figure 2. Monthly average partial ozone columns and temperatures on 440 K (black lines), 500 K (blue lines), and 600 K (red lines) isentropes in the Antarctic polar vortex in September (first and second panels) and October (third and fourth panels), respectively. The ozone data are obtained from the ozonesonde measurements for 1986–2007, the temporally and spatially coincident temperatures are calculated by using the NCEP temperatures. The correlation coefficients are calculated between temperatures on 440 K and 500 K surfaces and between 440 K and 600 K surfaces.

the September and October time periods. This strong vertical coherence of temperature enables temperature on the 440 K surface to be used to capture most of the variations in total column ozone that are associated with dynamical variability.

[18] Figure 3 shows the measurements of ozone in layers centered on the 440 K isentrope from SAGE II, HALOE, and ozonesondes, and measurements of total ozone from the Dobson/Brewer network. The measurements of total ozone (middle) were separated into three regions: vortex core (black dots), collar (blue dots), and outside the vortex (red dots). As expected, the collar region is located between 55° and 65°S equivalent latitude, with ozone abruptly decreasing toward the South Pole [see also *Bodeker et al.*, 2002]. Measurements of HCl from HALOE are also shown (Figure 3, bottom). The transition to enhanced levels of HCl in October is indicative of substantially reduced levels of ClO_x and reduced rates of chemical destruction of ozone in the vortex core. To obtain better coverage over the entire vortex region for the 1979 to 2007 time period, we have primarily relied on the ground-based Dobson/Brewer ozone observations (Figure 3, middle), which provide coverage

that is about 5 to 10 times denser than the SAGE II and ozonesonde measurements.

4. Temperature-Ozone Relationships

[19] Figure 4 shows daily total ozone columns (black dots) and temperatures on the 440 K surface (blue dots) for September (Figure 4, left) and October (Figure 4, right), in the vortex core (Figure 4, top) and in the collar region (Figure 4, bottom). There are substantial year-to-year variations in monthly mean ozone, especially in the vortex core, that are associated with year-to-year variations in monthly mean temperatures.

[20] Figure 5 shows the relationship between ozone residuals and temperature residuals, for data grouped into two time periods: 1979 to 1991 (prior to the onset of loss saturation) and 1994 to 2007 (subsequent to the onset of loss saturation). Residuals are defined by subtracting, from the raw data shown in Figure 4, the linear trend in ozone and temperature for the two time periods used in the trend analysis: 1979 to 1996 and 1997 to 2007. In other words, the ozone and temperature residuals for year 1994 shown in Figure 5 represent the deviation of the data for this year

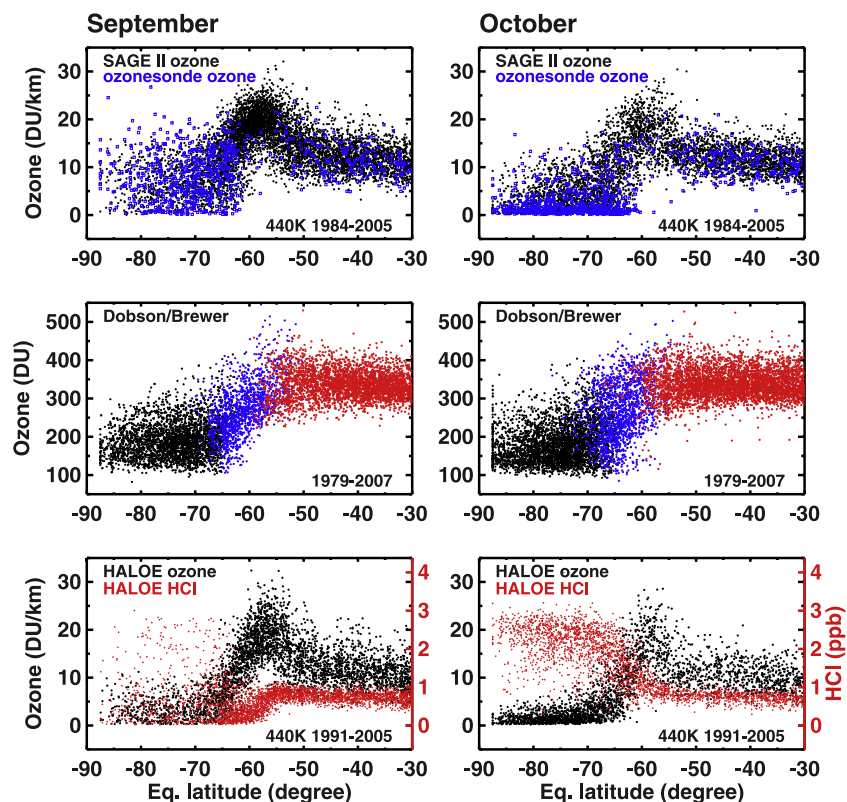


Figure 3. Ozone in equivalent latitude in (left) September and (right) October: from the top to the bottom, SAGE II (black dots) and ozonesonde (blue dots) measurements for 1984–2005, ground-based Dobson/Brewer measurements for 1979–2007, and HALOE measurements for 1991–2005. The SAGE, HALOE, and ozonesonde partial ozone columns are estimated on the 440 K isentrope. The Dobson/Brewer total ozone columns are separated into three regions: vortex core (black dots), collar (blue dots), and outside the vortex (red dots). The HALOE HCl mixing ratios are also shown by red dots (bottom).

from the linear trend in ozone and temperature over the 1979 to 1996 time period. We note also that polar ozone depletion has led to stratospheric cooling because of the strong contribution of ozone to the UV heating of this region of the atmosphere [e.g., *WMO*, 2007, Chapter 4]. The use of detrended residuals results in our analysis being insensitive, to first order, to this geophysical process.

[21] Ozone and temperature residuals are tightly correlated. This relation, noted by numerous prior studies [*Newman et al.*, 2004; *Huck et al.*, 2005], is commonly used to arrive at a time series for polar ozone that accounts for year-to-year variability induced by transport variations [*Newman et al.*, 2006], and is likely caused by both transport and chemical effects [*Huck et al.*, 2005]. As noted earlier, we use temperature at the 440 K potential temperature level, but temperature anomalies are well correlated at various isentropic levels in the vortex. Data in the core of the vortex in September have been restricted to geographic latitudes equatorward of 65°S because during this time period, the dependence of ozone depletion on temperature is relatively weak in many portions of the vortex core due to the coexistence of air masses with and without significant sunlight exposure during the month [*Hoppel et al.*, 2005]. Furthermore, temperature variability may be indicative of the presence of unmixed air parcels with different dynamical histories [*Manney et al.*, 1994]. The geographic latitude

has been averaged over 5 days, using calculated backward trajectories, to approximately account for the recent solar illumination history of the air parcels. No filtering is applied to any of the other data in Figure 5.

[22] For the data collected prior to the onset of loss saturation (1979 to 1991) in the vortex core and collar region, the ozone and temperature residuals have correlation coefficients of 0.73 and 0.92 for September and correlation coefficients of 0.93 and 0.89 for October. Figure 5 also shows the ozone and temperature residuals for 1994 to 2007 (blue triangles). Similar slopes in the September ozone versus temperature residual data are observed for data collected during both time periods. In October (both the vortex core and collar), the slope of residual ozone versus residual temperature is less steep for the 1994 to 2007 time period. This is almost certainly related to the more frequent occurrence of near-zero ozone values in the 1994 to 2007 time period.

[23] The above result differs from that shown by *Solomon et al.* [2005, Figure 5], who suggested that the slope of the relation between ozone and temperature at 70 hPa changed over time, going from less steep to more steep and more variable in recent years. We believe this is because *Solomon et al.* [2005] did not remove the long-term changes in ozone, mostly caused by variations in halogen loading. This difference resulted in visually different relationships between

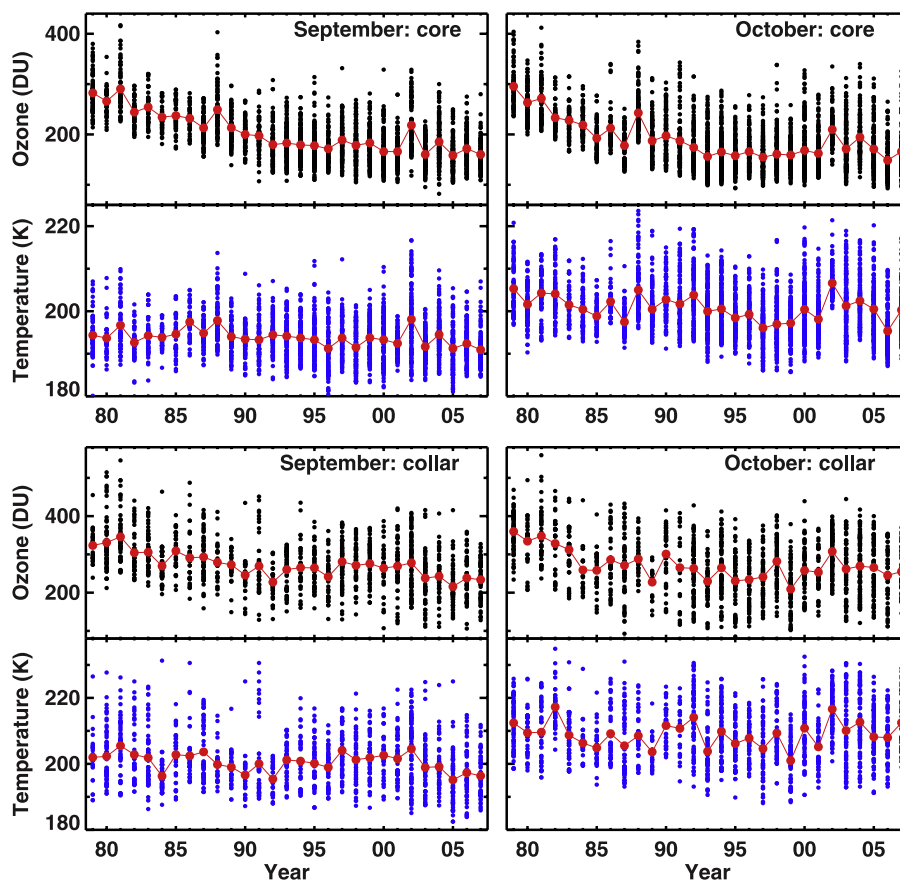


Figure 4. Ground-based Dobson/Brewer total ozone columns (black dots) and temperatures on 440 K (blue dots) for (left) September and (right) October in the vortex core (first and second panels) and in the collar region (third and fourth panels), respectively. The monthly averages for each ozone and temperature time series are shown with red dots.

temperature and ozone, for various time periods, which was amplified by their use of a logarithmic scale for ozone mixing ratio.

[24] Figure 6 shows our calculation of ozone (on a linear scale) and temperature at 70 hPa, for different time periods and observing stations, after removing the trends from the data (see caption). The October ozone after 1990 has a similar dependence on temperature as the ozone between 1960 and 1990, but shows a weak dependence on temperature after 1990 when ozone mixing ratios at 70 hPa are low. This change in ozone sensitivity to variations in temperature is expected because less ozone in October permits little additional ozone loss [Tilmes *et al.*, 2006]. In fact, the red dots and crosses in Figure 6 clearly show the limiting effects of saturation on ozone loss.

5. Loss Saturation Effects

5.1. Loss Saturation in Column Ozone

[25] Ozone equivalent anomalies are defined as the variations in ozone that are attributable to dynamical perturbations [Yang *et al.*, 2005]. Hereafter, anomaly refers to the difference between a measurement and the long-term climatological mean of the particular quantity, over the relevant time period. Ozone equivalent anomalies are calculated from the slopes of monthly mean ozone column residuals versus temperature residuals for 1979 to 1991 (Figure 5),

multiplied by the temperature anomaly (temperature minus climatological monthly mean value) for a particular month. Because the temperature trends for 1979–2007 are very small in the Antarctic polar vortex (Figure 4; see also WMO [2007, Figure 4.2]), the ozone equivalent anomalies are almost same as the ozone equivalent residuals. In order to compare with measured ozone residuals, ozone equivalent residuals are estimated by using temperature residuals:

$$\Delta O_3 \text{ EQUIVALENT RESIDUAL} = \beta^* \Delta T \quad (1)$$

where $\Delta T = T - \omega_T$ (temperature trend) and β is the slope of ozone residual versus temperature residual (Figure 5). Removal of these ozone equivalent residuals from the actual ozone time series then illuminates the long-term changes in ozone due to variations in stratospheric halogen loading. As noted in section 4, residual refers to a measurement minus its long-term trend.

[26] Ozone occasionally reaches near zero levels in the Antarctic vortex during spring [Hofmann *et al.*, 1997; Solomon *et al.*, 2005]. This effect is most common near 16–18 km (about 440 K) (see Figures 3 and 6). Because loss saturation has occurred more often in recent years, a flattening of the trend in total column ozone due to loss saturation could be erroneously interpreted as being due to changes in halogen loading.

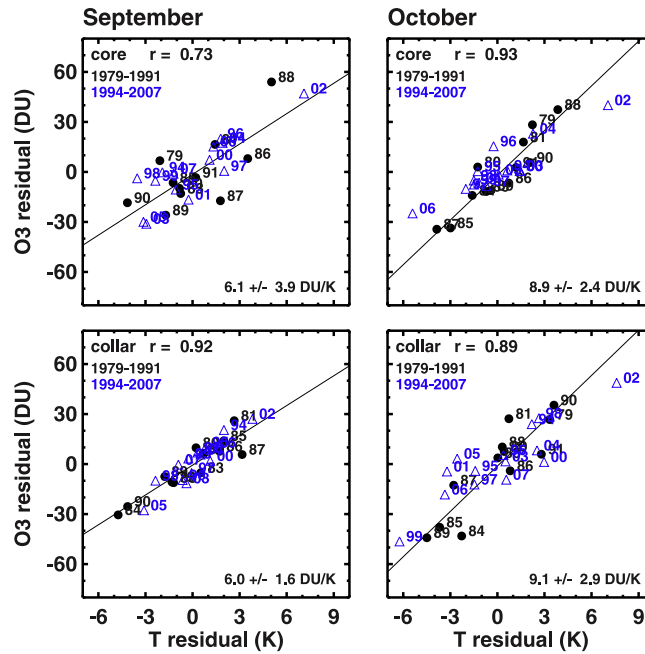


Figure 5. Temperature residuals on 440 K versus ozone column residuals for September (left) and October (right) (top) in the vortex core and (bottom) in the collar region, where residuals are calculated by removing the 1979–1996 trend line from each ozone and temperature time series in Figure 4. The temperature versus ozone residuals for 1994–2007, after removing trends for 1979–1996 and 1997–2007, are also shown with blue triangles for comparison. The slopes in DU/km $\pm 2\sigma$ and correlation coefficients are therefore estimated by using the residuals for 1979–1991, and they are provided in Figures 5 (bottom right) and 5 (top left), respectively.

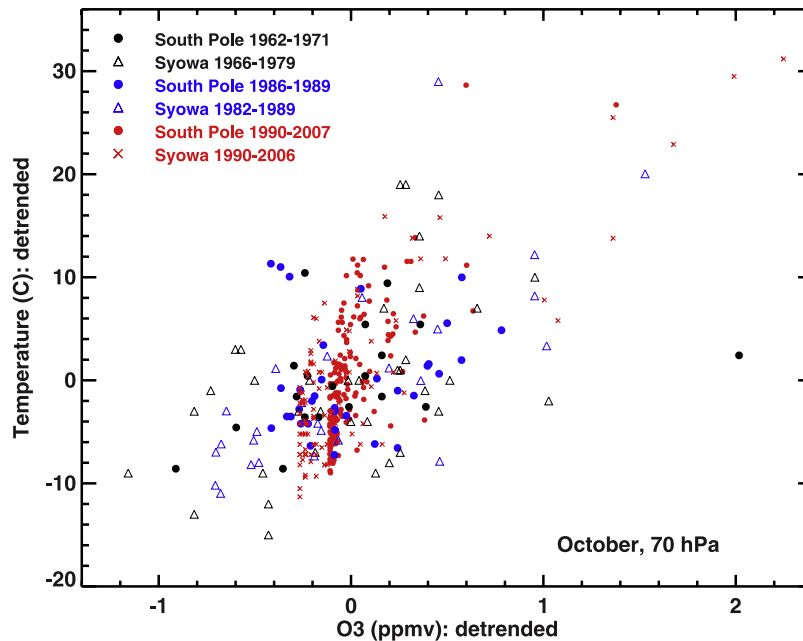


Figure 6. Scatterplot of October ozone mixing ratios with temperatures at 70 hPa. The data are obtained from the ozonesonde measurements at South Pole (solid circles) and Syowa (open triangles and crosses) over three different time periods. Note that the ozone mixing ratios are on a linear (not logarithmic) scale. The ozone mixing ratios and temperatures for 1979–1996 are detrended, and the data before 1979 and after 1997 have had their mean values subtracted.

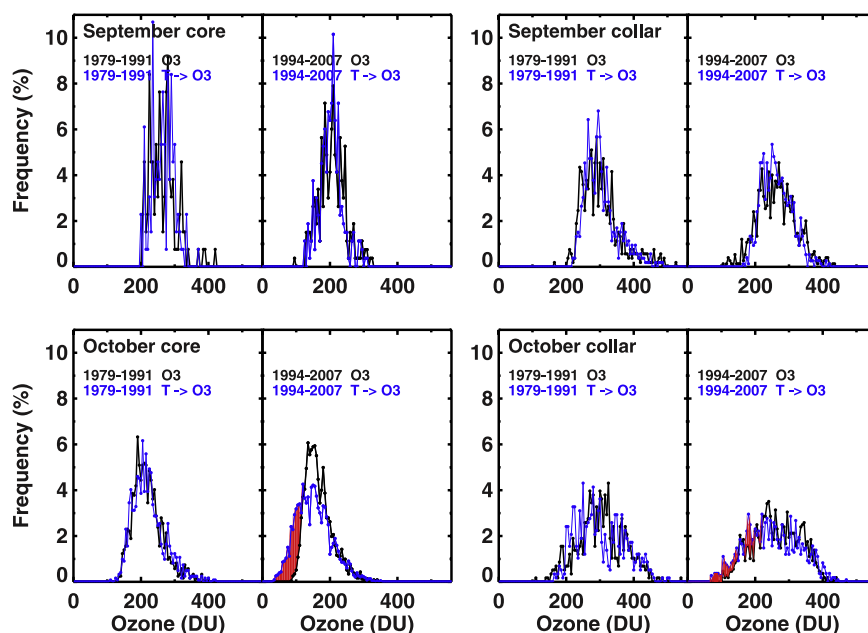


Figure 7. Frequency distribution in 5-DU intervals for the Dobson/Brewer total ozone columns for (top) September and (bottom) October (left) in the vortex core and (right) in the collar region during two different periods 1979–1991 and 1994–2007. The frequency distributions for temperature residuals have been converted to ozone units (ozone equivalent residuals) and are shown in blue to compare with those for the measured ozone in black. The mean ozone value is added to each residual to see the actual ozone level. The frequency distributions for the measured ozone have shorter tails toward the lower values in October 1994–2007 than do for the ozone equivalent residuals derived from temperature. The slopes of monthly means of ozone versus temperature residuals for 1979–1991 (i.e., before there was any substantial saturation) shown in Figure 5 are used to produce the ozone equivalent residuals for both 1979–1991 and for 1994–2007.

[27] To quantify the magnitude of saturation effects, we compare frequency distributions of ozone equivalent residuals to measured ozone residuals (Figure 7). Ozone equivalent residuals represent how much column ozone would have been present in the atmosphere, if ozone had responded to a variation between ozone and temperature in a manner based on atmospheric measurements made before the onset of loss saturation. Trends have been removed from both frequency distributions shown in Figure 7. We expect no difference in the upper tails of the frequency distribution of the ozone residual and the ozone equivalent residual because high ozone levels do not undergo loss saturation. By matching these upper tails, saturation will appear as the difference between the frequency distribution of the ozone residual (real data) and the ozone equivalent residual (reconstructed ozone) in the low ozone part of the distributions, because the reconstructed ozone is based on the slope between ozone and temperature acquired prior to 1992 (the onset of loss saturation).

[28] The frequency distributions of daily measured ozone column residuals and the ozone equivalent residuals are overlaid in Figure 7 for 1979–1991 and 1994–2007, for both the vortex core and collar regions. Because of the filtering of the September data in the vortex core, previously mentioned in section 4, relatively few data are available for this region (Figure 7, top left). It is noteworthy that the frequency distributions of the ozone equivalent residuals mostly replicate the distributions of the measured ozone residuals, except for the region of the distribution when

ozone column is small. The region where these two distributions differ, marked by red in Figure 7, is the signature of loss saturation. Conversely, the nearly identical frequency distributions of actual measured ozone and ozone equivalent residuals in the core and collar regions for September suggest that loss saturation has almost no effect during this month. Even though rapid ozone loss occurs during September, ozonesonde measurements indicate the abundance of ozone between ~ 12 and 22 km is always a measurable, positive value during September and that ozone first reaches zero at the start of October [e.g., Hofmann *et al.*, 1997, Figure 3].

[29] In October for the 1994–2007 period, loss saturation results in the mean of the measured total ozone column residuals being larger than the mean of the ozone equivalent residuals. Matching the upper tails of the two frequency distributions for this time period results in a mean difference of ~ 13 DU for the total ozone column in the vortex core during October. The red shading in Figure 7 (bottom left) illustrates the difference between these two frequency distributions. This difference does not change much if the matching range is varied from the highest 25% of the frequency distribution to the highest 15%. The 13 DU difference in mean column ozone is postulated as the amount of additional ozone loss that would have occurred in the core of the vortex, during October, if not for loss saturation. On the basis of the ~ 170 DU mean level of total ozone in the core of the vortex during October, the loss

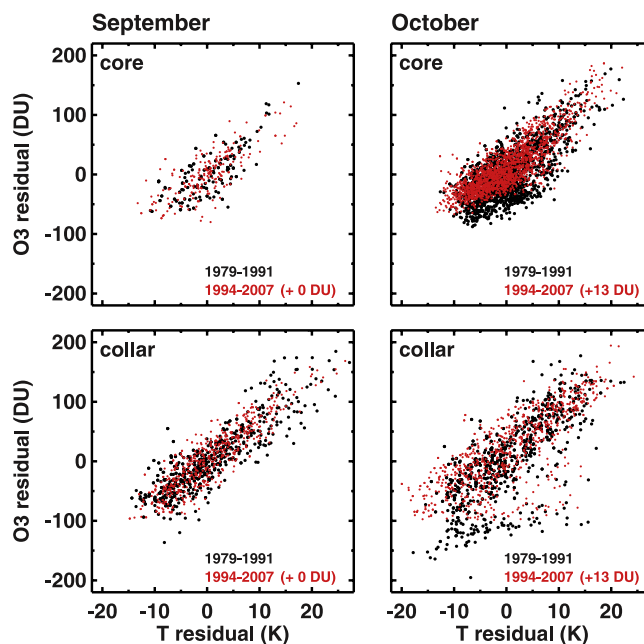


Figure 8. Same as Figure 5 but using daily ozone column residuals and temperature residuals on the 440 K isentrope for 1979–1991 (black dots) and 1994–2007 (red dots). Thirteen DU have been added to the October ozone for 1994–2007 in the vortex core and collar region to provide an overlapping comparison with the October ozone for 1979–1991.

saturation effect enhances the ozone column by approximately 8% in 1994–2007.

[30] The loss saturation effect in the collar region for October is shown by the red shaded area in Figure 7 (bottom right). The effect of loss saturation on column ozone in the vortex collar is similar to what was seen for the core. Even though the red area in Figure 7 (bottom right) appears to be smaller than that in Figure 7 (bottom left), the red shading for the collar extends to higher values of ozone. On the basis of the difference between the two distributions, we estimate ozone columns were again about 13 DU higher (or $\sim 5\%$ of the total column) in the collar region compared the columns that would have resulted if loss saturation had not occurred.

[31] The loss saturation effect estimate of 13 DU in the October collar region is larger than the value of <5 DU derived in our earlier study, which used SAGE II ozone measurements at $60\text{--}70^\circ\text{S}$ [Yang *et al.*, 2005]. This difference is likely to be caused by inclusion of all the SAGE II ozone data in the geographic latitudes between 60° and 70°S by Yang *et al.* [2005]. The difference between these two estimates of loss saturation are small and do not affect the scientific conclusions of either study.

[32] Figure 8 also illustrates the saturation effect by comparing scatterplots of ozone versus temperature residuals for 1979–1991 (black dots) with data for 1994–2007 (red dots). As in Figure 5, mean levels and linear trends were removed from the raw data using values for these quantities from the 1979–1996 and 1997–2006 time periods, respectively. Figure 8 confirms, to a first approximation, that the slopes of ozone versus temperature residuals are linear and that these slopes are similar, in September, for data collected during the 1979–1991 and 1994–2007 time periods. Hence, there is no evidence for loss saturation during September.

[33] Figure 8 provides another view of the evidence for ozone loss saturation during October. The ozone residuals during October for the 1994–2007 time period are smaller than the residuals for the 1979–1991 period. To quantify the amount of loss saturation in October, the measurements of total ozone in the October core and collar region obtained for 1994–2007 have been shifted upward by 13 DU, based on the estimate of loss saturation from the ozone equivalent residuals described above. The good overall agreement between the October residuals for 1979–1991 (black dots) and 1994–2007 (red dots), suggests 13 DU is the amount by which, on average, column ozone has been affected by loss saturation during October. In October, the sharp edge to the bottom portion of the red 1994–2007 data is due to loss saturation.

[34] In the October collar region (Figure 8, bottom right), most of the ozone residuals lie along the same temperature-ozone relation observed in the collar during September. However, a few ozone residuals lie far below the values expected from the September relationship. These low values of ozone appear to be characteristic of the vortex core. These data points may have been improperly assigned to the collar region because the polar vortex weakens or breaks up as the Antarctic spring progresses, which results in small-scale PV features that are difficult to resolve using the relatively coarse NCEP analysis. Indeed, most outliers in Figure 8 (bottom right) were measured in mid to late October. Because of the difficulty in defining the location of the polar vortex and presences of fewer data points, the loss saturation estimate for the October collar region would likely be more uncertain than the estimate for the October core.

[35] If there are significant uncertainties in the NCEP temperatures (i.e., uncertainties on order of several K), least

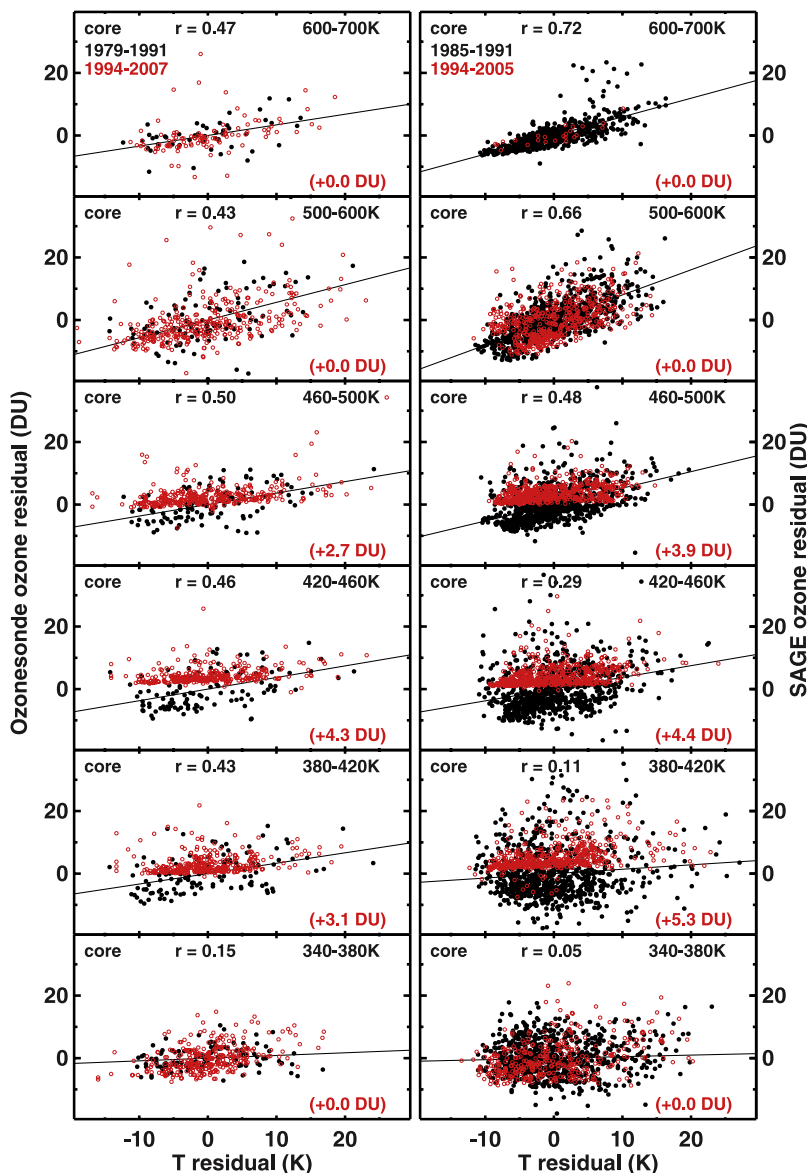


Figure 9. Temperature versus ozone residuals obtained from the (left) ozonesonde and (right) SAGE II measurements in the October vortex core, (from bottom to top) at 340–380 K, 380–420 K, 420–460 K, 460–500 K, 500–600 K, and 600–700 K surfaces, respectively. Residuals for 1979–1991 (black dots) are calculated by removing the 1979–1996 (or 1985–1996 for SAGE II) trend line from each monthly average ozone and temperature time series. The correlation coefficients are estimated by using the residuals for 1979–1991 (or 1985–1991). The temperature versus ozone residuals for 1994–2007 (or 1994–2005 for SAGE II), after removing trends for 1979–1996 and 1997–2007, are shown with red open circles. The mean differences in ozone values between black and red dots (shown in red) are added to each ozone residual for 1994–2007 to provide an overlapping comparison with the ozone residuals for 1979–1991 (or 1985–1991 for SAGE II).

squares fitting would tend to underestimate the slope of ozone versus temperature for the daily data shown in Figure 8 [e.g., *Johnston*, 1984, chapter 10]. In order to reduce uncertainties in ozone and temperature, the slopes of ozone versus temperature used to derive the ozone time series anomalies were based on regressions of monthly average ozone and temperature (Figure 5), rather than slopes derived from the daily data (Figure 8). Indeed, for the 1979–1991 time period, the slopes estimated by the least square fitting using the data in Figure 5 are 6.1, 6.0,

8.9, and 9.1 DU/K for the September core, September collar, October core, and October collar regions, respectively, while the slopes estimated using the daily data in Figure 8 are 5.7, 6.1, 5.6, and 6.6 DU/K, respectively. Note that the difference is largest in the October core, which is where saturation effects are largest.

5.2. Saturation Effect in Individual Layers

[36] We now quantify loss saturation in individual atmospheric layers, using profiles of ozone measured by ozone-

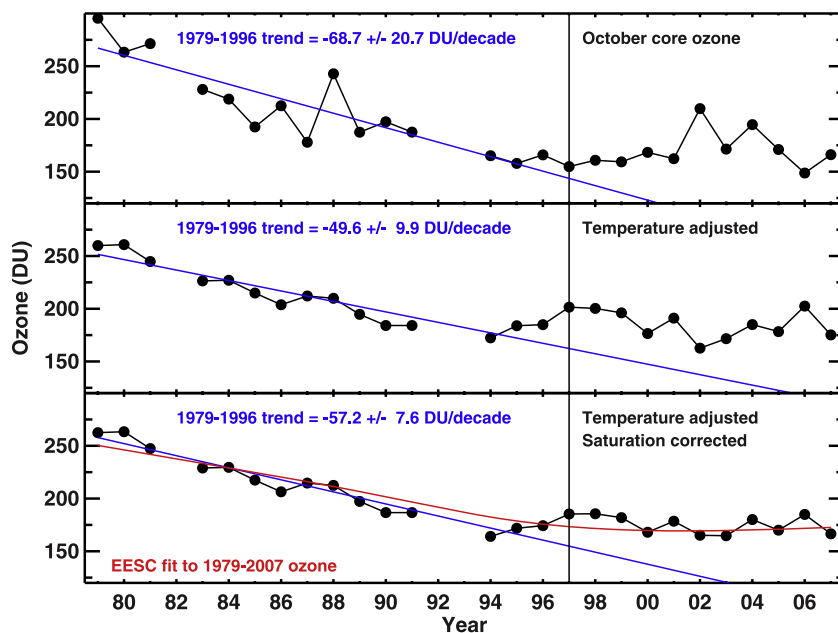


Figure 10. Monthly averaged Dobson/Brewer total column ozone in the October core. (top) Observed ozone, (middle) effect of having removed the effects of monthly mean temperature variations from the 1979–2007 ozone data, and (bottom) additional effects of adjustments for loss saturation in the 1994–2007 ozone data. The black line indicates the ozone trend calculated from observations for 1979–1996 and forecasted linearly afterward. Linear trends and 95% confidence intervals for 1979–1996 are listed in DU/decade. The red lines show the EEASC fits to the 1979–2007 ozone data.

sondes and SAGE II. The saturation estimates for various layers are summed and compared to the estimates for loss saturation of total column ozone found in section 5.1 (which were calculated using ground-based measurements).

[37] Figure 9 shows plots of ozone residuals versus temperature residuals, for partial ozone columns calculated on various potential temperature surfaces (as indicated). All data are for the core of the vortex in October. Data from ozonesondes and SAGE II appear in Figures 9 (left) and 9 (right) respectively. The time periods of the data are the same as used for Figures 5, 7, and 8. The calculation of ozone and temperature residuals (i.e., data minus linear trend for the time periods prior to and subsequent to the minimum in the second derivative of EEASC) is also the same as described in section 4.

[38] Loss saturation appears as the almost horizontal lower boundaries of the red data points (1994–2007 time period) for the atmospheric layers 380–420 K (14–16 km), 420–460 K (16–18 km), and 460–500 K (18–20 km) shown in Figure 9. This feature is apparent for both the ozonesonde and SAGE II data. There is no distinct difference between scatterplots of red and black dots below 380 K and above 500 K, suggesting these potential temperature levels correspond to the lower and upper boundaries of the loss saturation in the vortex core. Applying the same procedure illustrated in Figure 7 to derive the saturation effect, we calculate that the saturation effect raises the ozonesonde partial columns by 3.1, 4.3, and 2.7 DU for the 380–420, 420–460, and 460–500 K levels, respectively. The saturation estimates for the SAGE II partial columns are 5.3, 4.4, and 3.9 DU for the same levels (all numerical values are also given in Figure 9). The total saturation effect between 380 and 500 K is estimated to be 10.1 DU from the

ozonesonde data and 13.6 DU from the SAGE II measurements. These estimates are similar, and both agree quite well with the ~ 13 DU estimate that resulted from our analysis of the ground-based data.

6. Temperature-Adjusted and Saturation-Corrected Ozone Column Trends

[39] To estimate the effect on ozone of long-term variations in stratospheric halogen loading, it is first necessary to account for the effects of year-to-year temperature fluctuations and loss saturation. Figure 10 illustrates the steps used to obtain the long-term change in ozone, for the vortex core during October, which will be compared to changing amounts of stratospheric halogens. Figure 10 (top) shows the time series of total column ozone measured in the core of the vortex during October by the Dobson/Brewer network. The temperature effect is removed from the entire ozone time series (1979–2007) by using the linear temperature versus ozone residuals relationship for 1979–1991 (Figure 5). This process results in the time series of ozone shown in Figure 10 (middle), which represents a time series for ozone that has been adjusted to account for variations due to meteorological conditions. Since we have used the temperature versus ozone residuals relation acquired before the onset of loss saturation, this relation is likely to overcorrect the temperature dependence of ozone for the 1994–2007 time period. Because of loss saturation, low temperature would not have reduced ozone as much as expected from the relationship. The next step is quantitative representation of loss saturation in the ozone time series.

[40] In section 5.1, an average value for the loss saturation effect, over the 1994–2007 time period, was derived.

We would expect that as saturation effects increase, the sensitivity of ozone to temperature would decrease. Figures 5, 6, and 9 show analyses of residual ozone versus temperature, which is consistent with this expectation. We also expect that loss saturation would be sensitive to temperature for specific years, with colder conditions leading to more chemical loss (more polar stratospheric clouds leading to more chlorine activation) and also representing a more isolated vortex (less ozone transported into the vortex) [e.g., Huck *et al.*, 2005, and references therein]. The magnitude of loss saturation for the individual years in the 1994–2007 time period is assumed to be directly proportional to the monthly averaged temperatures, with more loss saturation occurring in cold years and less loss saturation in warm years. We also assume no loss saturation in 2002, the anomalously warm Antarctic spring. The loss saturation effect for each October is estimated from the deviation of each monthly averaged temperature from the monthly mean temperature in 2002, with the average of the loss saturations for the 1994–2007 time period being set equal to 13 DU. Figure 10 (bottom) shows the ozone time series after adjustment for both temperature effects (all data) and saturation effects (1994–2007 time period).

[41] Figure 10 (bottom) also shows the time series for EEASC (same relation as shown by the red solid line in Figure 1), which has been fitted to the ozone columns for the 1979–2007 time period. The EEASC fit represents a constant, multiplicative factor applied to the EEASC curve, such that the residual between the ozone time series and fit are minimized in a least squares sense. The column ozone time series, adjusted both for temperature variations and loss saturation (Figure 10, bottom) is well described by the EEASC time series. This result suggests that once variations in ozone due to meteorological conditions and loss saturation have been quantified, the resulting ozone time series is controlled strongly by stratospheric halogen loading.

[42] Unusually low values of ozone were observed in the core of the vortex during 2006 (Figure 10, top). Also, unusually low temperatures were observed in 2006 (Figure 4, top right). On the basis of the difference between the data points for 2006 shown in Figure 10 (top and middle), we estimate that the low temperatures of 2006 would have led to a 54 DU reduction in column ozone compared to values that occur for typical temperature conditions. However, because of loss saturation, the actual ozone column in the core of the vortex during October 2006 was only ~ 36 DU lower than that which would have occurred for a typical year (difference between 2006 data in Figure 10 (middle and bottom)). Interestingly, the data point for 2006, once the temperature and loss saturation effect have been accounted for, is indistinguishable from data collected during other years in the 1994–2007 time period. The positive ozone anomaly associated with warm temperatures in September 2002, as seen in Figure 10 (top), is also no longer noticeable in Figure 10 (bottom).

[43] Figure 11 (left) shows the time series of total ozone columns after the effects of meteorological conditions and loss saturation have been removed, for the core of the vortex during September and October (Figure 11, first panel) and for the collar region of the vortex, also for September and October (Figure 11, fourth panel). As noted in section 4, data in the core of the vortex during September are

restricted to geographic latitude equatorward of 65°S . No filtering is applied to the data in the second, third, and fourth panels of Figure 11. Data collected during October for the years 1994 to 2007, when loss saturation is evident (section 5), are shown both with (black solid circles) and without (blue open triangles) consideration of the correction for loss saturation (Figure 11, second and fourth panels). For the rest of the discussion, we consider only the total ozone columns that have been corrected for loss saturation.

[44] We now estimate linear trends for the 1979–1996 time period, which will later be compared to the data collected in the 1997–2007 time period. The trend estimates (black lines) and 95% confidence limits are -49.2 ± 14.8 , -57.2 ± 7.6 , -34.4 ± 6.8 and -61.0 ± 11.1 DU/decade for the September vortex core, October vortex core, September vortex collar, and October vortex collar regions, respectively (numerical values also given on Figure 11). These trend estimates are consistent with the estimates of -45 to -53 DU/decade for the 60 – 70°S geographic latitude region given by Yang *et al.* [2005] (same time period) and of -59 ± 12 DU/decade for the Antarctic ozone minima given by WMO [2003, Chapter 3], for the 1979–2000 time period.

[45] The black solid lines in Figure 11 represent the downward, linear trend in the total ozone columns found for the 1979–1996 time periods. The lines have been extended beyond 1996. Comparison of these extended lines to the total ozone columns for the 1997–2007 time period shows systematically positive values of ozone relative to the propagation of the linear trend. This comparison suggests that the decline in ozone slowed in 1997, which was identified in section 1 (and Figure 1) as the time when such a change would be evident, based on the second derivative of EEASC.

[46] We now turn to a more formal statistical analysis. The cumulative sum (CUSUM) of residuals quantifies systematic departures of ozone from the trend line [Reinsel, 2002; Newchurch *et al.*, 2003; Yang *et al.*, 2006]. Each value in the CUSUM time series (Figure 11, right) represents the cumulative difference of all the anomalies, with respect to the 1979–1996 trend line, for the year in question plus all earlier years. Since the reference line is the linear trend for the 1979–1996 period, the CUSUM points for 1979 to 1996 are close to zero (deviations from zero represent scatter about the trend line). The CUSUM points for 1997 and later years are positive, indicating the departure from the prior, downward trend. This behavior is readily apparent from the ozone data points shown in Figure 11 (left). The CUSUM method allows for formal determination of uncertainties, which is an important component of the identification of recovery (i.e., the changes must be statistically significant). The 95% confidence limits for an unbiased random walk about the projected trend line appear as the blue traces, where the limits also include uncertainties in the trend model estimates. The confidence limits were computed as described by Yang *et al.* [2006, Appendix]. At the end of the time period (i.e., for 2007), all of the CUSUM values lie outside of the 95% uncertainty envelopes. This indicates that the ozone time series (following removal of year-to-year variations due to temperature and adjustment for loss saturation) is following a trend line after 1997 that is different from the 1979–1996 trend

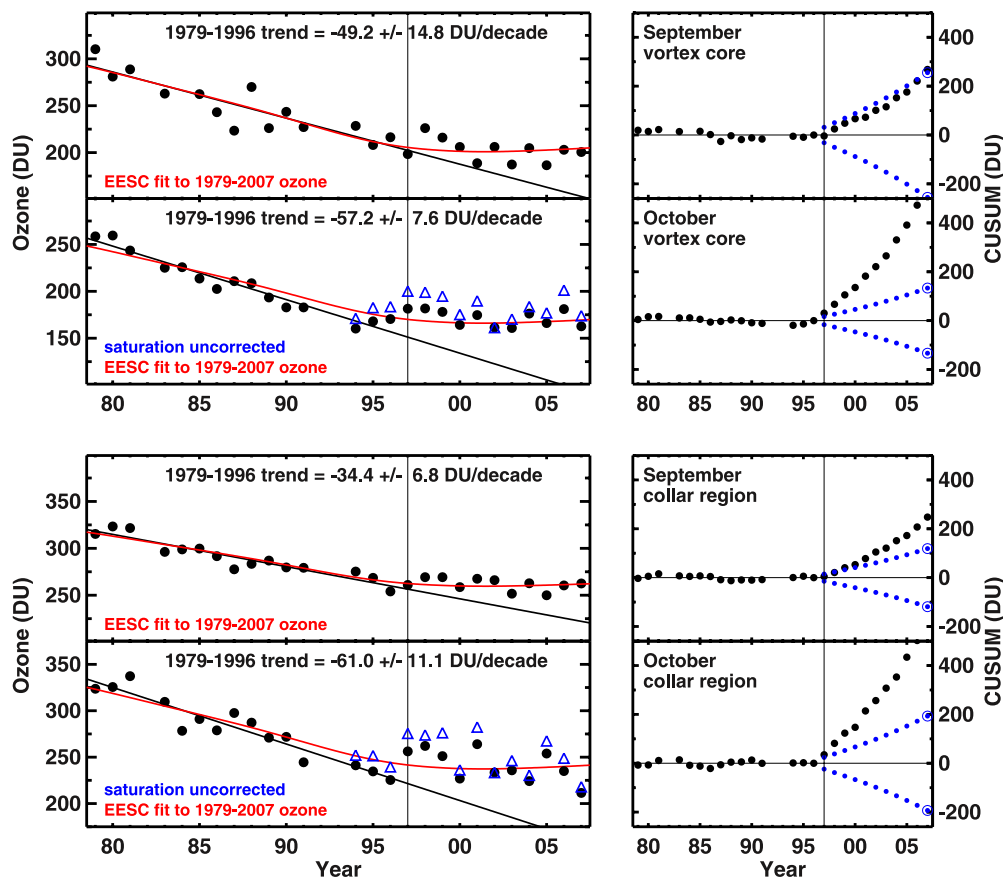


Figure 11. (left) Temperature-adjusted ozone time series and (right) cumulative sum (CUSUM) of the difference between these ozone columns and the long-term trend line (i.e., residuals from the trend line) in DU for Dobson/Brewer total ozone columns: (first panel) September vortex core, (second panel) October vortex core, (third panel) September vortex collar, and (fourth panel) October vortex collar. The temperature-adjusted ozone time series are obtained by subtracting the ozone equivalent residuals from the ozone time series. The black line indicates the ozone trend calculated from observations for 1979–1996 and forecasted linearly afterward. Linear trends and 95% confidence intervals for 1979–1996 are listed in DU/decade. In the October vortex core (second panel) and collar region (fourth panel), the ozone values for 1994–2007 are shown without loss saturation correction (blue triangles) and with loss saturation correction (black circles). The red lines show the EESC fits to the 1979–2007 temperature-adjusted ozone time series. The blue lines in Figure 11 (right) indicate the 95% confidence envelopes of departure from natural variability and trend model uncertainty.

line at greater than the 95% confidence level. In other words, all of the ozone time series given in Figure 11 exhibit a statistically significant change in slope in 1997, which is precisely where such a change is expected, based on the minimum of the second derivative of EEASC.

[47] The red lines in Figure 11 show fits of EEASC to the ozone time series, using data collected for the entire 1979 to 2007 time period. The fits have been computed in the same manner as described for Figure 10. The close visual correspondence of the shape of these fit curves to the total ozone columns, for the vortex core and collar, September and October, indicates that the long-term evolution of Antarctic ozone is well described by the temporal variations in the abundance of stratospheric halogen loading. We therefore conclude that measurements since 1997 indicate Antarctic ozone, within both the core and collar region, is in its first stage of recovery, as defined by *WMO* [2007, Chapter 6]. The data exhibit a statistically significant slow-

ing of the previous decline, in a manner that is clearly attributable to changes in the abundance of ozone depleting substances.

7. Conclusions

[48] We have analyzed ground-based, ozonesonde, and satellite observations of ozone within the core and collar regions of the Antarctic ozone hole obtained over the time period 1979 to 2007. Our focus has been to determine if Antarctic ozone has undergone the first stage of recovery due to reductions in the abundance of stratospheric halogens brought about by the Montreal Protocol and its amendments. The first stage of recovery is defined as the occurrence of a statistically significant reduction in the rate of ozone decline that is clearly attributable to changes in the abundance of ozone depleting substances [WMO, 2007, Chapter 6].

[49] Variations in Antarctic ozone were related to changes in stratospheric halogen loading using a version of Equivalent Effective Stratospheric Chlorine specific to the Antarctic vortex, termed EEASC [Newman *et al.*, 2006]. We showed that the second derivative (with respect to time) of EEASC reached a sharp, well-defined minimum in early 1997, indicating 1997 is when the rate of decline of Antarctic ozone would be expected to exhibit the largest amount of change.

[50] Much of our analysis centered on the development of quantitative methods to account for year-to-year fluctuations in ozone due to dynamical variability and to adjust ozone time series for the effect of ozone loss saturation. Ozone loss saturation refers to the phenomena that as ozone abundance approaches zero, the “leveling off” of column ozone could be due to the fact that the atmosphere, in certain parts of the ozone hole, has run out of ozone that can be depleted.

[51] The slope between residuals (i.e., deviations from long-term trends) of temperature and ozone column was used to compute ozone anomaly time series for which year-to-year variations in ozone due to meteorological conditions were removed. Ozone anomaly time series specific to the core and collar of the Antarctic vortex, for the months September and October, all exhibit a compact, near linear decline from 1979 to 1996 and little change from 1997 to 2007.

[52] The quantification of ozone loss saturation was a strong focus of the analysis. The ground-based Dobson/Brewer ozone column data showed that during October, loss saturation has been apparent since 1994 in the core and collar regions of the Antarctic vortex (loss saturation actually first became apparent in 1992, but data for 1992 and 1993, as well as data for 1982, are not used in this analysis due to the effect on ozone of volcanically enhanced aerosols for these 3 years [Hofmann *et al.*, 1994; Bevilacqua *et al.*, 1997; Nardi *et al.*, 1997; Hofmann *et al.*, 1997]). Loss saturation was also shown to be evident in ozonesonde and SAGE II observations between 380 and 500 K potential temperature (14–20 km). We used a comparison of the frequency distribution of measured ozone versus the distribution expected from a reconstructed relation based on ozone and temperature residuals to estimate that the effect of loss saturation on total column ozone during October was ~13 DU, for both the vortex core and collar regions. In other words, the actual column of ozone observed during October since 1994, in both the vortex core and collar, was on average ~13 DU larger than would have been observed had ozone responded linearly to variations in temperature (i.e., had ozone levels been hypothetically allowed to become negative). We also estimated similar abundances of loss saturation based on integration of estimates from an analysis of ozone profiles measured by ozonesondes and SAGE II. We found no evidence for loss saturation in September, consistent with previous studies of the ozone hole [Hofmann *et al.*, 1997].

[53] We then formed ozone time series for which perturbations due to variations in meteorological conditions and loss saturation had been taken into account. These four time series represented data collected in the core and collar of the vortex, during September and October. The four ozone time series were all shown to exhibit a change in slope after

1997, the expected break point based on the second derivative of EEASC. A CUSUM analysis of these time series demonstrated a decline in the rate of ozone loss, since 1997, statistically significant at the 95% confidence level. All of the time series were shown to be well-described by the temporal variation in EEASC over the 1979 to 2007 time period. We conclude, therefore, that Antarctic ozone has undergone the first stage of recovery, due to the decrease in halogen loading over the past decade.

[54] Our study demonstrates that changes in stratospheric halogen loading initiated by the Montreal Protocol and its amendments has led to a quantifiable, positive impact on Antarctic springtime ozone since 1997. Even though the rate of increase of stratospheric halogens has declined significantly, the actual amount of halogens in the stratosphere has declined only slightly relative to its peak in the modern era. The first stage of recovery as defined by WMO [2007] means that chemical loss of Antarctic ozone is no longer continuing to worsen. Interestingly, the Antarctic vortex now appears to be in a state where year-to-year variations in total column ozone are driven primarily by variations in temperature and meteorological conditions, as was the case for the abnormally high levels of column ozone observed in 2002 and the unusually low amounts of column ozone measured in 2006. The high ozone observed in 2002 and the low ozone observed in 2006 were both shown to be consistent with the amount of halogens present at those times, once the temperature anomaly and corresponding loss saturation effects had been taken into account. Antarctic ozone will continue to be affected by year-to-year variations in temperature [Huck *et al.*, 2005], but the overall trend in column ozone is expected to generally follow variations in halogen loading [Austin and Wilson, 2006; Newman *et al.*, 2006]. The next stage of recovery defined by WMO [2007], marked by an increase in Antarctic total column ozone that is clearly attributable to reduced abundances of halogens will likely not be identified until several decades in the future because of the slow rate of decline of EEASC (Figure 1).

[55] **Acknowledgments.** We thank P. Newman for providing a Web site that we have used to calculate EEASC and for many helpful discussions. Dobson/Brewer total ozone and ozonesonde ozone data were provided by the Swiss Meteorological Service with additional data available at the World Ozone and Ultraviolet Data Center (WOUDC). Dobson total ozone data at Vernadsky (Faraday) and Halley were obtained from the British Antarctic Survey (BAS). Ozonesonde data at South Pole were provided by NOAA/ESRL. The NCEP temperature data were obtained from NOAA-CIRES/CDC. E.-S. Yang was supported by NASA at Georgia Tech for the majority of this work. NASA also provided the majority of support to the other authors for this research. Work at the Jet Propulsion Laboratory, California Institute of Technology, was performed under contract with the National Aeronautics and Space Administration. We thank three anonymous reviewers for providing many detailed, thoughtful comments that led to substantial revisions and a significantly improved paper. We note that our paper represents the complete data record from the remarkable SAGE and HALOE instruments. SAGE I commenced observations in 1979 and SAGE II ceased operating on 22 August 2005. HALOE ceased operating on 14 December 2005. The SAGE I/II and HALOE instruments documented the relationship between CFCs and polar ozone depletion, details of the microphysics of polar stratospheric cloud formation, and the physical (denitrification) and chemical (chlorine activation) effect of PSCs. The data record provided by these instruments played an important role in quantifying the effect of human activity on the polar ozone depletion that led to the passage of the Montreal Protocol and its amendments, which have essentially eliminated the production of CFCs and related species. It is a strong testament to the respective instrument teams

that both SAGE II and HALOE remained operational long enough to observe the beginning of the recovery of the Antarctic ozone hole.

References

- Allen, D. R., R. M. Bevilacqua, G. E. Nedoluha, C. E. Randall, and G. L. Manney (2003), Unusual stratospheric transport and mixing during the 2002 Antarctic winter, *Geophys. Res. Lett.*, *30*(12), 1599, doi:10.1029/2003GL017117.
- Anderson, J., J. M. Russell III, S. Solomon, and L. E. Deaver (2000), Halogen Occultation Experiment confirmation of stratospheric chlorine decreases in accordance with the Montreal Protocol, *J. Geophys. Res.*, *105*(D4), 4483–4490, doi:10.1029/1999JD901075.
- Austin, J., and R. J. Wilson (2006), Ensemble simulations of the decline and recovery of stratospheric ozone, *J. Geophys. Res.*, *111*, D16314, doi:10.1029/2005JD006907.
- Bevilacqua, R. M., et al. (1997), POAM II ozone observations in the Antarctic ozone hole in 1994, 1995 and 1996, *J. Geophys. Res.*, *102*(D19), 23,643–23,657, doi:10.1029/97JD01623.
- Bodeker, G. E., H. Struthers, and B. J. Connor (2002), Dynamical containment of Antarctic ozone depletion, *Geophys. Res. Lett.*, *29*(7), 1098, doi:10.1029/2001GL014206.
- Butchart, N., and E. E. Remsburg (1986), The area of the stratospheric polar vortex as a diagnostic for tracer transport on an isentropic surface, *J. Atmos. Sci.*, *43*(13), 1319–1339, doi:10.1175/1520-0469(1986)043<1319:TAOTSP>2.0.CO;2.
- Chipperfield, M. P., and J. A. Pyle (1998), Model sensitivity studies of Arctic ozone depletion, *J. Geophys. Res.*, *103*(D21), 28,389–28,403, doi:10.1029/98JD01960.
- Farman, J. C., B. G. Gardiner, and J. D. Shanklin (1985), Large losses of total ozone in Antarctica reveal seasonal ClO_x/NO_x interaction, *Nature*, *315*, 207–210, doi:10.1038/315207a0.
- Froidevaux, L., et al. (2006), Temporal decreases in upper atmospheric chlorine, *Geophys. Res. Lett.*, *33*, L23812, doi:10.1029/2006GL027600.
- Hofmann, D. J., and S. J. Oltmans (1993), Anomalous Antarctic ozone during 1992: Evidence for Pinatubo volcanic aerosol effects, *J. Geophys. Res.*, *98*(D10), 18,555–18,562, doi:10.1029/93JD02092.
- Hofmann, D. J., S. J. Oltmans, J. M. Harris, S. Solomon, T. Deshler, and B. J. Johnson (1992), Observation and possible causes of new ozone depletion in Antarctica in 1991, *Nature*, *359*, 283–287, doi:10.1038/359283a0.
- Hofmann, D. J., S. J. Oltmans, J. A. Lathrop, J. M. Harris, and H. Vömel (1994), Record low ozone at the South Pole in the spring of 1993, *Geophys. Res. Lett.*, *21*(6), 421–424, doi:10.1029/94GL00309.
- Hofmann, D. J., S. J. Oltmans, J. M. Harris, B. J. Johnson, and J. A. Lathrop (1997), Ten years of ozonesonde measurements at the south pole: Implications for recovery of springtime Antarctic ozone, *J. Geophys. Res.*, *102*(D7), 8931–8943, doi:10.1029/96JD03749.
- Hoppel, K., R. Bevilacqua, T. Canty, R. Salawitch, and M. Santee (2005), A measurement/model comparison of ozone photochemical loss in the Antarctic ozone hole using Polar Ozone and Aerosol Measurement observations and the Match technique, *J. Geophys. Res.*, *110*, D19304, doi:10.1029/2004JD005651.
- Huck, P. E., A. J. McDonald, G. E. Bodeker, and H. Struthers (2005), Interannual variability in Antarctic ozone depletion controlled by planetary waves and polar temperature, *Geophys. Res. Lett.*, *32*, L13819, doi:10.1029/2005GL022943.
- Huck, P. E., S. Tilmes, G. E. Bodeker, W. J. Randel, A. J. McDonald, and H. Nakajima (2007), An improved measure of ozone depletion in the Antarctic stratosphere, *J. Geophys. Res.*, *112*, D11104, doi:10.1029/2006JD007860.
- Jiang, Y., Y. L. Yung, and R. W. Zurek (1996), Decadal evolution of the Antarctic ozone hole, *J. Geophys. Res.*, *101*(D4), 8985–8999, doi:10.1029/96JD00063.
- Johnston, J. (1984), *Econometric Methods*, 3rd ed., McGraw-Hill, New York.
- Lee, A. M., H. K. Roscoe, A. E. Jones, P. H. Haynes, E. F. Shuckworth, M. W. Morrey, and H. C. Pumphrey (2001), The impact of the mixing properties within the Antarctic stratospheric vortex on ozone loss in spring, *J. Geophys. Res.*, *106*(D3), 3203–3211, doi:10.1029/2000JD900398.
- Manney, G. L., R. W. Zurek, A. O'Neill, and R. Swinback (1994), On the motion of air through the stratospheric polar vortex, *J. Atmos. Sci.*, *51*, 2973–2994, doi:10.1175/1520-0469(1994)051<2973:OTMOAT>2.0.CO;2.
- Massom, R. A., P. Reid, S. Barreira, and S. Stammerjohn (2008), Sea ice extent and concentration, in *State of the Climate in 2007*, edited by D. H. Levinson and J. J. Lawrimore, *Bull. Am. Meteorol. Soc.*, *89*, spec. suppl., S105–S106.
- Nardi, B., T. Deshler, M. E. Hervig, and L. D. Oolman (1997), Spring 1996 and 1997 ozonesonde measurements over McMurdo Station, Antarctica during spring 1994 and 1995, *Geophys. Res. Lett.*, *24*(3), 285–288, doi:10.1029/97GL00035.
- Nardi, B., W. Bellon, L. D. Oolman, and T. Deshler (1999), Spring 1996 and 1997 ozonesonde measurements over McMurdo Station, Antarctica, *Geophys. Res. Lett.*, *26*(6), 723–726, doi:10.1029/1999GL900083.
- Nash, E. R., P. A. Newman, J. E. Rosenfield, and M. R. Schoeberl (1996), An objective determination of the polar vortex using Ertel's potential vorticity, *J. Geophys. Res.*, *101*(D5), 9471–9478, doi:10.1029/96JD00066.
- Newchurch, M. J., E.-S. Yang, D. M. Cunnold, G. C. Reinsel, J. M. Zawodny, and J. M. Russell III (2003), Evidence for slowdown in stratospheric ozone loss: First stage of ozone recovery, *J. Geophys. Res.*, *108*(D16), 4507, doi:10.1029/2003JD003471.
- Newman, P. A., S. R. Kawa, and E. R. Nash (2004), On the size of the Antarctic ozone hole, *Geophys. Res. Lett.*, *31*, L21104, doi:10.1029/2004GL020596.
- Newman, P. A., E. R. Nash, S. R. Kawa, S. A. Montzka, and S. M. Schauffler (2006), When will the Antarctic ozone hole recover?, *Geophys. Res. Lett.*, *33*, L12814, doi:10.1029/2005GL025232.
- Perlwitz, J., S. Pawson, R. L. Fogt, J. E. Nielsen, and W. D. Neff (2008), Impact of stratospheric ozone hole recovery on Antarctic climate, *Geophys. Res. Lett.*, *35*, L08714, doi:10.1029/2008GL033317.
- Reinsel, G. C. (2002), Trend analysis of upper stratospheric Umkehr ozone data for evidence of turnaround, *Geophys. Res. Lett.*, *29*(10), 1451, doi:10.1029/2002GL014716.
- Solomon, S. (1999), Stratospheric Ozone Depletion: A Review of Concepts and History, *Rev. Geophys.*, *37*(3), 275–316, doi:10.1029/1999RG900008.
- Solomon, S., R. W. Portmann, T. Sasaki, D. J. Hofmann, and D. W. J. Thompson (2005), Four decades of ozonesonde measurements over Antarctica, *J. Geophys. Res.*, *110*, D21311, doi:10.1029/2005JD005917.
- Son, S.-W., L. M. Polvani, D. W. Waugh, H. Akiyoshi, R. Garcia, D. Kinnison, S. Pawson, E. Rozanov, T. G. Shephard, and K. Shibata (2008), The impact of stratospheric ozone recovery on the southern hemisphere westerly jet, *Science*, *320*, 1486–1489, doi:10.1126/science.1155939.
- Tilmes, S., R. Müller, J.-U. Grooß, R. Spang, T. Sugita, H. Nakajima, and Y. Sasano (2006), Chemical ozone loss and related processes in the Antarctic winter 2003 based on Improved Limb Atmospheric Spectrometer (ILAS)-II observations, *J. Geophys. Res.*, *111*, D11S12, doi:10.1029/2005JD006260.
- Waugh, D., and T. Hall (2002), Age of stratospheric air: Theory, observations, and models, *Rev. Geophys.*, *40*(4), 1010, doi:10.1029/2000RG000101.
- Weatherhead, E. C., and S. B. Andersen (2006), The search for signs of recovery of the ozone layer, *Nature*, *441*(7089), 39–45, doi:10.1038/nature04746.
- World Meteorological Organization (WMO) (2003), Scientific assessment of ozone depletion: 2002, *Global Ozone Res. Monit. Proj. Rep.* *47*, 498 pp., Geneva.
- World Meteorological Organization (WMO) (2007), Scientific assessment of ozone depletion: 2006, *Global Ozone Res. Monit. Proj. Rep.* *50*, 572 pp., Geneva.
- Yang, E.-S., D. M. Cunnold, M. J. Newchurch, and R. J. Salawitch (2005), Change in ozone trends at southern high latitudes, *Geophys. Res. Lett.*, *32*, L12812, doi:10.1029/2004GL022296.
- Yang, E.-S., D. M. Cunnold, R. J. Salawitch, M. P. McCormick, J. Russell, I. I. I. Joseph, M. Zawodny, S. Oltmans, and M. J. Newchurch (2006), Attribution of recovery in lower-stratospheric ozone, *J. Geophys. Res.*, *111*, D17309, doi:10.1029/2005JD006371.
- D. M. Cunnold, School of Earth and Atmospheric Sciences, Georgia Institute of Technology, 311 Ferst Drive, Atlanta, GA 30332-0340, USA.
- M. P. McCormick and J. M. Russell III, Center for Atmospheric Sciences, Hampton University, 23 Tyler Street, Hampton, VA 23668, USA.
- M. J. Newchurch, Atmospheric Science Department, University of Alabama in Huntsville, 320 Sparkman Drive, Huntsville, AL 35805, USA. (mike@nsstc.uah.edu)
- S. J. Oltmans, NOAA Earth System Research Laboratory, 325 Broadway, Boulder, CO 80305, USA.
- R. J. Salawitch, Department of Atmospheric and Oceanic Sciences, University of Maryland, 2403 Computer and Space Science Building, College Park, MD 20742, USA.
- E.-S. Yang, ESSC, University of Alabama in Huntsville, 320 Sparkman Drive, Huntsville, AL 35805, USA.
- J. M. Zawodny, NASA Langley Research Center, MS 475, Hampton, VA 23681, USA.